The Terminal (Catalytic) Adenosine of the HIV LTR Controls the Kinetics of Binding and Dissociation of HIV Integrase Strand Transfer Inhibitors

David R. Langley,[‡] Himadri K. Samanta,[§] Zeyu Lin,[§] Michael A. Walker,[||] Mark R. Krystal,[§] and Ira B. Dicker*[,§]

Departments of Computer Assisted Drug Design, Virology, and Medicinal Chemistry, Bristol-Myers Squibb Research & Development, Wallingford, Connecticut 06492

Received July 22, 2008; Revised Manuscript Received September 22, 2008

ABSTRACT: Specific HIV integrase strand transfer inhibitors are thought to bind to the integrase active site, positioned to coordinate with two catalytic magnesium atoms in a pocket flanked by the end of the viral LTR. A structural role for the 3′ terminus of the viral LTR in the inhibitor-bound state has not previously been examined. This study describes the kinetics of binding of a specific strand transfer inhibitor to integrase variants assembled with systematic changes to the terminal 3′ adenosine. Kinetic experiments are consistent with a two-step binding model in which there are different functions for the terminal adenine base and the terminal deoxyribose sugar. Adenine seems to act as a "shield" which retards the rate of inhibitor association with the integrase active site, possibly by acting as an internal competitive inhibitor. The terminal deoxyribose is responsible for retarding the rate of inhibitor dissociation, either by sterically blocking inhibitor egress or by a direct interaction with the bound inhibitor. These findings further our understanding of the details of the inhibitor binding site of specific strand transfer inhibitors.

HIV integrase (IN)[1]is absolutely required for productive HIV infection and, as such, is an attractive anti-HIV drug target (*1*). HIV IN strand transfer inhibitors (STIs), which selectively target the strand transfer activity of IN, possess potent anti-HIV activity in cell culture (*2*−*5*), and the first one of these, raltegravir (*6*), has been approved for use in treatment-experienced patients while a second, Elvitegravir (*7*), is progressing through clinical trials.

The virus-encoded IN protein catalyzes two essential activities in the viral life cycle: 3′-processing (3′-P) and strand transfer (*8, 9*). The 3′-P reaction cleaves the final two bases, a 3′-GT dinucleotide, from the 3′ ends of the viral LTRs. The strand transfer activity catalyzes the concerted insertion of each of the two viral 3′ ends into the host genome with a five base pair separation. To accomplish this, the IN complexes simultaneously position the two 3′ hydroxyls of the LTRs for nucleophilic attack onto the phosphodiester bonds of complementary strands of genomic DNA (*10*), leading to the initial strand transfer products. Cellular enzymes are thought to repair the five base pair gap leading to the final integration product.

Specific STIs of the diketoacid class and isosteres selectively inhibit the strand transfer strand step catalyzed by HIV IN (*4, 11*−*13*). The assembly of IN onto the viral LTR stimulates the high affinity binding of STIs, suggesting that the binding pocket for these inhibitors is derived from a specific structural arrangement of the nucleoprotein complex (*3*−*5, 14*−*21*). Published models of HIV IN (*19, 22*) suggest that these specific STIs bind to the IN active site in a pocket flanked by the end of the LTR such that the diketoacid moiety, or its mimic, is positioned to coordinate with both of the catalytic magnesium atoms (*23*−*25*) (*14, 19, 22, 26*−*29*). Amino acid substitutions which confer resistance to STIs cluster around the IN active site (*30*−*37*), and changes to the 5′ end of the LTR reduce the affinity of a specific STI for its binding site (*16*). Published models do not address the issue of the precise placement of the 3′ terminus of the viral LTR in the inhibitor-bound state. However, it can be proposed that such inhibitors should bind in a pocket which was formerly occupied by the 3′ GT dinucleotide prior to its endonucleolytic cleavage by the 3′-P function of IN, leaving the terminal A[1] as the last base after processing (Figures 1, 2A).

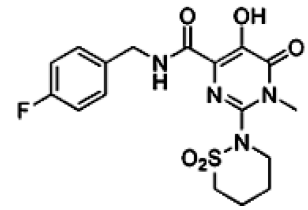

FIGURE 1: HIV integrase strand transfer inhibitor **1**.

We previously reported that IN complexes efficiently assembled onto an LTR altogether lacking the terminal 3′ adenosine (dC[2] OH, Table 1). A specific STI binds to these complexes with relatively high affinity, indicating that the terminal adenosine is dispensable, per se, for binding (*16*). Here we report a detailed kinetic analysis of the binding of a specific STI to IN complexes prepared with defined changes at the terminal 3′ adenosine. These studies indicate that the terminal (catalytic) 3′ adenosine

* Corresponding author. Tel: 203-677-7736. Fax: 203-677-6088. E-mail Ira.Dicker@BMS.com.
[‡] Department of Computer Assisted Drug Design.
[§] Department of Virology.
[||] Department of Medicinal Chemistry.

[1] Abbreviations: IN, integrase; STI, strand transfer inhibitor; 3′-P, 3′-processing.

10.1021/bi801372d CCC: $40.75
Published on Web 11/08/2008

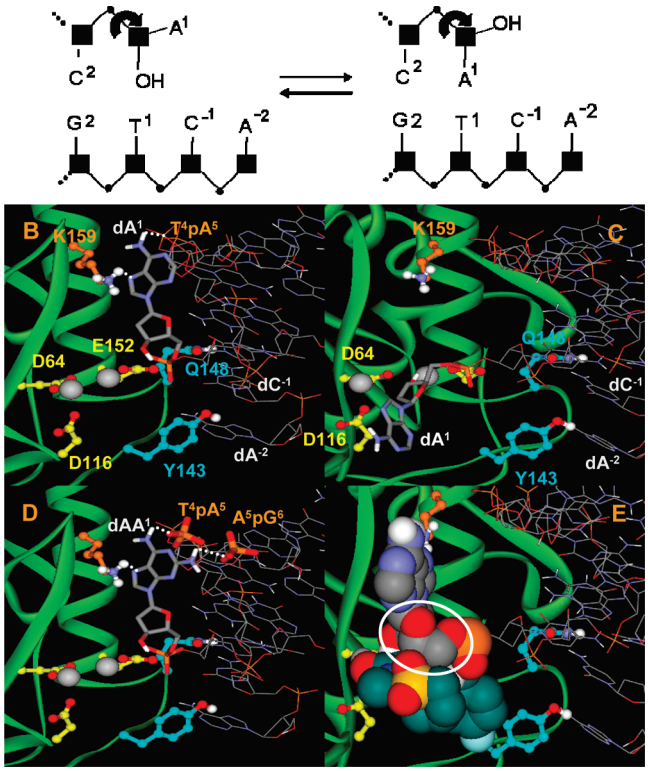

FIGURE 2: A. Sequence of the HIV U5 LTR terminus after 3′ processing. Boxes: deoxyribose sugars; circles: phosphates. The arrow depicts one of several hypothetical rotations of the terminal adenosine. B. CADD model of the IN active site in the "open" conformation showing dA^1 turned away from the inhibitor binding site and forming two hydrogen bonds (white dotted lines). C. CADD model of the IN active site in the "closed" conformation showing dA^1 turned toward the active site, blocking inhibitor access. D. CADD model showing dAA^1 in the "open" conformation and forming three hydrogen bonds. E. CADD model of the IN active site showing bound inhibitor packed against the sugar (circled) of A^1.

of the HIV LTR controls the kinetics of binding and dissociation of HIV IN STIs.

EXPERIMENTAL PROCEDURES

Materials. STI inhibitor **1** (IC_{50} in the *in vitro* strand transfer reaction of 15 nM (*16*)) and [^{3}H]-**1** (specific activity 28.6 cpm/fmol, 0.96×10^6 cpm/μL) were prepared by the Medicinal Chemistry Group at Bristol-Myers Squibb. Viral long terminal repeat (LTR) oligonucleotides were prepared for attachment to streptavidin-coated SPA PVT beads (Amersham), which were used in both strand transfer and [^{3}H]-**1** binding assays, as previously described (*16*). The LTRs were "preprocessed", i.e., they did not contain the 3′ terminal GT dinucleotide. Viral LTR duplexes (3′ terminal A^1 is bolded) were constructed based on the NL4−3 laboratory strain of HIV: (plus strand: 5′ biotin-ACCCTTTTAGTCAGTGTGGAAAATCTCTAGC^2**A**^{1} 3′; minus strand: 5′ ACTGCTAGAGATTTTCCACACTGACTAAAAG 3′. Oligonucleotides were prepared by Sigma-Genosys (Woodlands, TX), except for dC^2 pdS, which was prepared by TriLink BioTechnologies (San Diego). PVT scintillation proximity assay (SPA) beads were from Amersham Biosciences. The d-spacer and aminadenosine monomers were from Glen Research, Sterling, VA. Recombinant IN enzymes were purified from an NL4-3 clone, as previously described (*16*).

*Kinetics of [^{3}H]-**1** Binding and Dissociation.* A SPA format was used to measure the kinetics of binding of [^{3}H]-**1** to IN complexes assembled with the preprocessed LTR variants containing systematic changes to the terminal (3′) adenosine (*16*). LTR duplexes were prepared such that the 5′ end of the plus strand was synthesized with a biotin linker attached. An abasic site was engineered by substitution with a hydrolytically stable replacement of the deoxyribose base by a furanyl derivative. (Glen Research, Sterling, VA). Duplex LTRs were prepared as follows: 25 μL of the plus strand DNA (96 μM in TE) and 30 μL of the minus strand DNA (96 μM in TE) were combined with 145 μL of TE and annealed at 80 °C for 4 min and then allowed to slowly cool to 20 °C over a 60 min period. The viral (donor) LTR DNA duplexes were then attached, via the 5′ biotin linker on the plus strand, to streptavidin-coated SPA PVT beads (Amersham) as follows: SPA PVT beads (10 mg) were suspended in 0.2 mL of PBS. The suspension was then centrifuged at <5000*g* for 15 min. The supernatant was removed, and the pellet was resuspended with 0.2 mL of PBS/0.85 M NaCl and 21 μL of 12 μM duplex HIV LTR DNA. The LTR DNA was allowed to bind for 60 min at room temperature with gentle rocking, after which time 0.8 mL of TE was added. The mixture was then centrifuged at <5000*g* and resuspended in 0.8 mL of TE/50 mM NaCl. The beads were washed four additional times with TE/50 mM NaCl, each time centrifuging to remove unbound viral LTR DNA. The final pellet was resuspended in 0.2 mL of PBS and stored at 4 °C before use. SPA bead/LTR DNA/integrase enzyme complexes for 80 reactions were prepared as follows: 0.15 mL of bead/DNA complexes, 2.25 mL of SPA buffer [13.3 mM DTT, 32 mM MOPS pH 7.0, 0.067% NP40, 6.4% PEG, 25.6 mM $MgCl_2$, 12.8% (v/v) DMSO, and 100 mM NaCl], and IN (37 μg) were incubated at 37 °C. After 1.5 h, complexes were pelleted and resuspended with 2.4 mL of SPA buffer.

Kinetics were carried out in white 96-well microtiter plates (Corning, #3600) containing 40 μL of preformed IN complexes. A dilution series of [^{3}H]-**1** was prepared in buffer A, and 10 μL of each dilution was added to separate wells, in duplicate. Wells were read once every 30 s on a Topcount (Perkin-Elmer) scintillation counter. Dissociation of [^{3}H]-**1** was initiated by adding 10 μL of 100 μM (final concentration) unlabeled **1**. Kinetics were analyzed using Graphpad Prism, V5.03.

RESULTS

The Kinetics of [^{3}H]-1 Binding to IN are Relatively Slow. We first measured the dissociation constant, K_d, of [^{3}H]-**1** (*16*) to HIV IN complexes assembled with a WT preprocessed LTR (lacking the terminal 3′ GT dinucleotide), fitting the data to a single site binding model (eq 1).

$$E + L \underset{k_{on}}{\overset{k_{off}}{\rightleftharpoons}} EL, \qquad (1)$$

where $k_{obs} = k_{on}[\text{inhibitor}] + k_{off}$.

The apparent equilibrium dissociation constant, K_d (apparent), was 21 nM, as previously reported (*16*). To further characterize the binding of [^{3}H]-**1**, we measured the kinetics of binding and dissociation of [^{3}H]-**1**. Association curves were produced over a range of concentrations of [^{3}H]-**1** (0.6

Table 1: Rate Constants for the Binding of ^{3}H-**1** to INs Assembled with Changes to the Terminal Adenosine at 20° C[a]

no.	LTR[b]	k_1, μM^{-1} s^{-1} ($\times 10^{-2}$)	k_{-1}, s^{-1} ($\times 10^{-3}$)	k_2, s^{-1} ($\times 10^{-4}$)	k_{-2}, s^{-1} ($\times 10^{-4}$)	k_{on},[c] $\mu M^{-1}s^{-1}$ ($\times 10^{-1}$)	k_{off},[d] s^{-1} ($\times 10^{-4}$)	K_d (1)[e] nM	K_d (2)[f]	K_d (net)[g] nM	strand transfer IC_{50}, nM
1	dC^{2}pdA^1 (WT)	3.2	2.8	7.4	2.0	0.081	1.5	86.9	0.27	18.5	14
2	dC^{2}pdC^1	38	5.7	6.3	1.6	0.46	1.4	14.9	0.25	3.0	5.3
3	dC^{2}pdAA^1	16	1.9	3.6	1.3	0.32	1.0	12.1	0.36	3.2	1.1
4	dC^{2}pdS					6.3	3.6			0.56	2.6
5	dC^{2}OH					$\geq$2.0[h]	140			98[i]	N.A.
6	dC^{2}Op					$\geq$1.4[h]	42			30[i]	N.A.

[a] Data is fit to either a one- or two-step binding mechanism, as described in the text. N.A.: no strand transfer activity, p: phosphate, d: deoxy, S: dspacer, dAA: 2,6-diaminopurine 2′-deoxyriboside. [b] LTR variants as defined in the text. [c] k_{on} for rows 1, 2, and 3 following Bevilacqua et al. (*38*): $k_{on} \approx k_1 \times (k_2 + k_{-2})/(k_{-1} + k_2 + k_{-2})$. [d] k_{off} for rows 1, 2, and 3 following Bevilacqua et al. (*38*): $k_{off} \approx (k_{-1} \times k_{-2})/(k_{-1} + k_2 + k_{-2})$. [e] K_d (1) = k_{-1}/k_1. [f] K_d (2) = k_{-2}/k_2. [g] K_d (net) = k_{off}/k_{on}. [h] k_{on} was estimated from k_{off} and the equilibrium K_d. [i] k_d as described in the text.

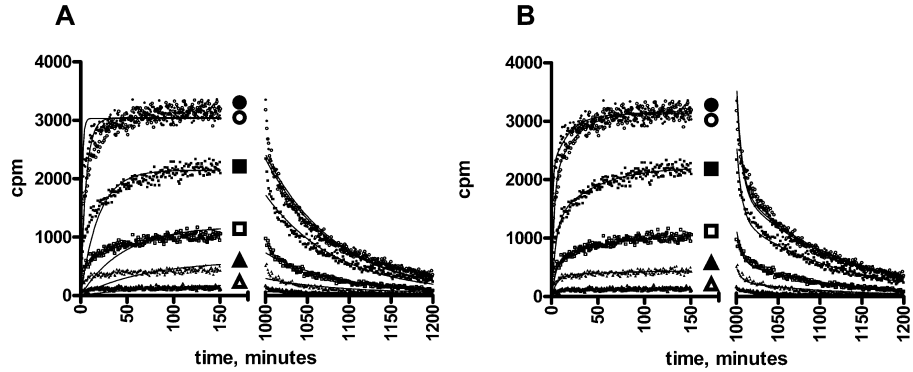

FIGURE 3: Association and dissociation kinetics of [^{3}H]-**1** binding to WT IN complexes at 20 °C. The kinetics of dissociation were monitored after adding a large molar excess of unlabeled **1**. [^{3}H]-**1** concentrations: Symbols are, as noted, next to the association and dissociation curves. Closed circles: 643 nM, open circles: 161 nM, closed boxes: 40 nM, open boxes: 10 nM, closed triangles: 2.5 nM, open triangles: 0.63 nM. A: Data fit to a single-step binding mechanism. B: Data fit to a two-step binding mechanism.

up to 643 nM). After equilibrium was reached, the kinetics of dissociation were monitored after adding a large molar excess of unlabeled **1**. The kinetic association data were first fit to a one-site binding model, proceeding via a single binding step (Figure 3A), giving the forward rate constant, k_{on}, and the reverse rate constant, k_{off} (eq 1). Inhibitor **1** associates and dissociates relatively slowly at 20 °C. The apparent second-order forward rate constant was 1.66×10^{-2} μM^{-1} s^{-1} and the apparent dissociation rate constant was $4.2 \pm 0.6 \times 10^{-4}$ s^{-1}. However, the global fit to this kinetic model is imperfect (Figure 3A). As might be expected from the figure, the correlation of the observed rate constants to the concentration of radiolabel is not perfectly linear (data not shown). The dissociation rate constant was measured directly, using a chase experiment with an excess of unlabeled **1**. A single monoexponential fit to the data provided a value for k_{off} which was 2.2-fold slower than that calculated from the simple global model using only the association binding data. Altogether, both the association and dissociation data fit far better to a biexponential equation, suggesting at least a two-step binding model. The association and dissociation data fit much better when globally fitted to a model (*38*) encompassing the formation of a lower affinity enzyme/ligand intermediate (EL*), via forward and reverse rate constants k_1 and k_{-1}, which then subsequently transitions to a higher affinity complex, EL, via rate constants k_2 and k_{-2} (eq 2 and Table 1).

$$E + L \underset{k_{-1}}{\overset{k_1}{\rightleftharpoons}} EL^* \underset{k_{-2}}{\overset{k_2}{\rightleftharpoons}} EL \qquad (2)$$

The averages of the rate constants obtained by simultaneous global fitting of two independent experiments to both the association and dissociation data are shown in Table 1, and representative curves are shown in Figure 3B. The initial complex has a dissociation constant, K_d (**1**), of 87 nM, while the final complex binds [^{3}H]-**1** 3.7-fold more tightly with a dissociation constant (K_d net) of 19 nM.

This two-step mechanism for the binding of **1** is consistent with a model in which the initial complex undergoes some kind of a time-dependent conformational change. The half-life for this secondary process could be estimated from the forward rate constant (7.4×10^{-4} s^{-1}) for the second binding step as 16 min at 20 °C. We hypothesized that this secondary process might involve a conformational rearrangement in the immediate vicinity of the inhibitor binding site due to the likely proximity of the 3′ terminal adenosine to the inhibitor binding and strand transfer active site. To this end, we modeled WT IN where dA^1 is turned away (designated as the "open conformation") from the active site (Figure 2B). This is hypothesized to be the predominant conformation before, during, and immediately following the 3′-processing reaction, possibly conforming to the intermediate which has recently been suggested by Pandey et al. (*39*). The major groove edge of dA^1 is proximal to K159, consistent with cross-linking results (*40*). Figure 2C shows WT IN, in which dA^1 has been rotated such that it occupies the active site. This "closed active site" is hypothesized to be the dominant conformation post 3′-processing, prior to and during strand transfer. To test this hypothesis we sought to determine whether the kinetics of inhibitor binding would be sensitive to changes at that site.

Changes to the 3′ Adenosine of the HIV LTR Alter the Kinetics of Inhibitor Binding. Simple replacements of the terminal adenine base by cytosine (C), thymine (T), or

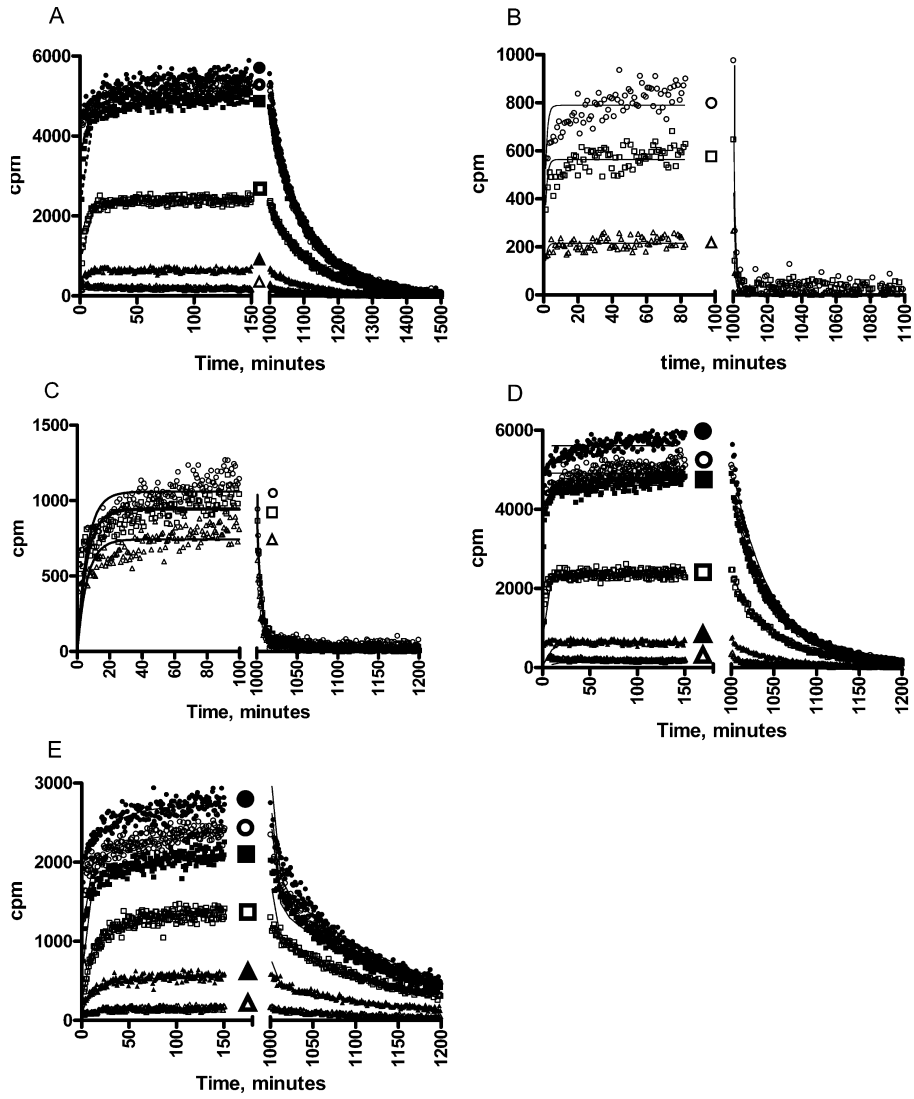

FIGURE 4: Association and dissociation kinetics of [^{3}H]-**1** binding to IN complexes assembled with variant LTRs at 20 °C. The kinetics of dissociation were monitored after adding a large molar excess of unlabeled 1. Data fit to a single site, two-step binding mechanism: (A) dC^2 pdC^1, (E) dC^{2}pdAA^1. Data fit to a single site, single-step binding mechanism: (B) dC^{2}pOH, (C) dC^2 Op, and (D) dC^2 pdS. Symbols are, as noted, next to the association and dissociation curves. [^{3}H] **1** concentrations: A, D and E: closed circles: 643 nM, open circles: 161 nM, closed boxes: 40 nM, open boxes: 10 nM, closed triangles: 2.5 nM, open triangles: 0.63 nM. B: open circles: 279 nM, open squares: 139 nM, open triangles: 35 nM; C: open circles: 150 nM, open squares: 75 nM, open triangles: 38 nM.

guanine (G) provided IN complexes which retained [^{3}H]-**1** binding and strand transfer activity. All three complexes possess approximately 25% of WT strand transfer activity, but the complex containing the cytosine replacement (dC^2 pdC^1 IN) had the highest relative affinity for [^{3}H]-**1** (*16*). High affinity binding was first quantified by determining the IC_{50} for inhibition of dC^{2}pdC^1 IN-mediated strand transfer activity by nonradiolabeled **1**. The IC_{50} was 5.3 nM, ~3-fold lower than that for the WT IN complex (Table 1, row 2). We then conducted a more detailed kinetic examination of dC^2 pdC^1 IN. In contrast to the relatively slow forward kinetics observed for the WT LTR (composite forward rate constant, k_{on}, 8.1×10^{-3} μM^{-1} s^{-1}), the forward kinetics for dC^2 pdC^1 IN were more rapid. Like WT, the data fit best to a two-step binding model (eq 2), but k_{on} (4.6×10^{-2} μM^{-1} s^{-1}) was 5.7-fold faster than WT (Table 1 and Figure 4A). The origin of the faster overall association rate was in the initial binding step, as the rate constant for the second step was similar to WT. The second-order initial forward rate constant, k_1, for dC^2 pdC^1 IN (3.8×10^{-1} μM^{-1} s^{-1}), was 12-fold faster than for WT (3.2×10^{-2} μM^{-1} s^{-1}). In contrast, the initial reverse rate constant, k^{-1}, was only marginally increased (5.7×10^{-3} s^{-1}, 2-fold faster than WT), providing overall dissociation kinetics which were slightly slower than WT (Figure 5). Thus, the increased affinity for the dC^2 pdC^1 complex is predominantly due to a more rapid formation of the initial lower affinity complex. We hypothesize that the faster formation of this initial complex is the result of a faster rate of interconversion of the open and closed complexes, respectively (Figures 2B and C) and/or a shift in the equilibrium between these conformers in favor of the open complex (Figure 2B). This may be due to the smaller size of the cytosine base, which renders it incapable of maintaining potential interactions with nearby amino acids which might stabilize the closed state.

We also compared the kinetics of binding of [^{3}H]-**1** to an IN complex assembled with an LTR containing the relatively conservative substitution of 2,6-diaminopurine 2′-deoxyriboside (dAA) in place of the 3′ adenine. This base contains an extra amino group at the 2-position of the purine,

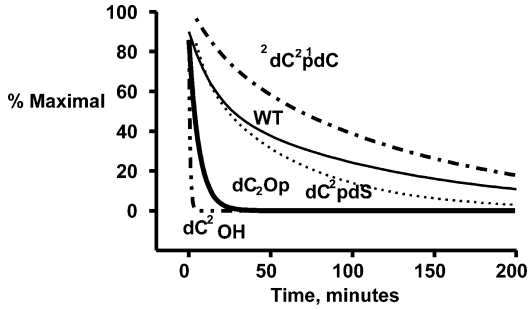

FIGURE 5: Dissociation of [^{3}H]-**1** from variant IN complexes. 643 nM [^{3}H]-**1** was allowed to bind to INs until equilibrium had been reached (600 min). Dissociation data was obtaining after adding 100 μM (final concentration) of unlabeled inhibitor 1. Data is normalized to percent maximal signal for each variant.

rendering it capable of forming additional hydrogen bonds with appropriate acceptors. One possibility suggested by modeling includes interactions of both amino groups of dAA with the phosphate groups between dT^4 and dA^5 and between dA^5 and dG^6 (Figure 2D) of the nonprocessed strand (numbering the 5′ terminal adenine as A^{-2}). In this case, k_1 for the formation of the initial complex was, like that for the dC^2 pdC^1 complex, faster than WT (5-fold), though 2.4-fold slower than that for dC^2 pdC^1 IN. The affinity of the initial complex (K_d (**1**)) was 12 nM, 7.2-fold lower than the initial complex of WT (87 nM). Overall, K_d (net) was 5.8-fold lower for the dAA change, vs WT, the result of the faster formation of EL* (eq 2). Thus, the kinetic profile of dC^2 pdAA^1 IN is similar to that of dC^2 pdC^1 IN.

To determine what components of the 3′ terminus were responsible for these altered kinetics, we measured the kinetics of binding of [^{3}H]-**1** to INs assembled with LTRs containing systematic deletions from the terminal adenosine. As shown in Figures 4B and 5, and Table 1, binding of [^{3}H]-**1** to IN assembled with the dC^2 OH LTR (deletion of the terminal adenosine, i.e., the adenine, its attached deoxyribose and intervening phosphate bridge) dramatically increased both the on (≥25-fold) and the off-rates (93-fold) for [^{3}H]-**1** binding. The forward rate constant was too rapid to be accurately measured using the scintillation proximity format but could be estimated from the equilibrium K_d and the reverse rate constant. The equilibrium K_d was calculated by fitting the data to a one-step binding model (eq 1). Despite the greatly accelerated kinetics vs WT, the overall affinity of [^{3}H]-**1** for the dC^2 OH IN complex (98 nM) was only reduced 5.3-fold versus WT. We interpret the faster association of [^{3}H]-**1** to the dC^2 OH complex as suggesting that removal of the terminal adenosine removes a block to the entry of the inhibitor to the active site, thus increasing the rate of inhibitor binding. On the other hand, the significantly faster dissociation kinetics indicates that some component of the terminal 3′ adenosine is no longer retarding the dissociation of the inhibitor from the active site.

To further dissect the role of the individual components of the adenosine on binding kinetics, we studied LTRs with partial deletions. We first studied complexes assembled with a terminally abasic LTR (dC^2 pdS). This LTR lacks a 3′ adenine but still contains a hydrolytically stable tetrahydrofuran (S = dspacer) (*16*) ring in place of the natural deoxyribose sugar at the 3′ terminus. The dC^2 pdS LTR IN catalyzed strand transfer with approximately 25% of WT activity (data not shown), similar to the catalysis of strand transfer by a terminally abasic site in the Mu A transposase (*41*). The IC$_{50}$ for inhibition of strand transfer activity of the dC^2 pdS complex by nonradiolabeled 1 was 2.6 nM, ~6-fold lower than that for the WT IN complex (Table 1), indicating tighter binding of **1** to the dC^2 pdS complex.

The kinetics of the binding and dissociation of [^{3}H]-**1** to the dC^2 pdS IN complex fit better to a one-step binding model (Figure 4D), in which the forward rate constant for binding of [^{3}H]-**1** was 78-fold faster than the composite k_{on} for WT (Table 1). These faster association kinetics indicate that the adenine base plays a specific and critical role in retarding the rate of inhibitor association toward WT IN. By contrast, the dissociation of inhibitor from dC^2 pdS IN was nearly as slow as WT (k_{off} increased only 2.4-fold over WT). This latter result indicates that the sugar, the sugar−phosphate, or the phosphate is predominantly responsible for the slow rate of inhibitor dissociation.

With a further truncation of the LTR, leaving only a terminal phosphate (dC^2 OP IN), the kinetics of association and dissociation of [^{3}H]-**1** were nearly as rapid as those from the dC^{2}OH IN complex (Table 1, row 5 and Figure 4B). Thus, the sugar, and not the bridging C^2-A^1 phosphate, per se, is responsible for the slow dissociation kinetics of this STI from the assembled IN complex (Figure 5). We hypothesize that the dA^1 sugar either interacts with the hydrophobic ring system of the STI (Figure 2E) or is positioned in such as way as to sterically retard inhibitor dissociation.

DISCUSSION

A large number of studies indicate that subsequent to the association of IN with the viral LTR termini, the IN 3′-P function endolytically cleaves the final two bases from the 3′ end (GT dinucleotide). The resulting terminal 3′ hydroxyl then acts as a nucleophile in a second enzymatic step, joining the 3′ end of the LTR with target double-stranded DNA (chromosomal DNA in the cell). The last base on the processed 3′ end of the LTR terminus is an adenine. To date, there has been no description of the detailed conformational arrangement of the DNA at the terminus of the viral LTR that gives rise to the inhibitor-bound state. However, base substitutions, cross-linking studies, molecular models (*17*−*22*), and resistance data converge on the idea that STIs bind near to the LTR terminus (reference *16* and references therein). A recent modeling paper places the integrase inhibitor within this structural context in detail (*42*). In particular, there is a paucity of information as to the role, if any, of the terminal adenosine in inhibitor binding. Also, there have been no published reports on the details of the kinetics of STI binding to HIV IN. Such information may usefully inform drug discovery efforts by helping to properly model the inhibitor-bound state.

This study made use of a SPA technique to measure binding kinetics. Binding kinetics measured by SPA methods have been reported to produce quantitatively comparable rate constants to those obtained by more traditional approaches. For example, the binding and dissociation rate constants (*43*) for [^{3}H]-nitroarginine binding to the N-terminal heme-binding domain of rat neuronal nitric oxide synthase were the same as those determined by inhibition of catalysis (*44*) or by a precipitation method (*45*). Also, the binding kinetics of a nonpeptide antagonist, [^{3}H]-SB-674042, to the human or-

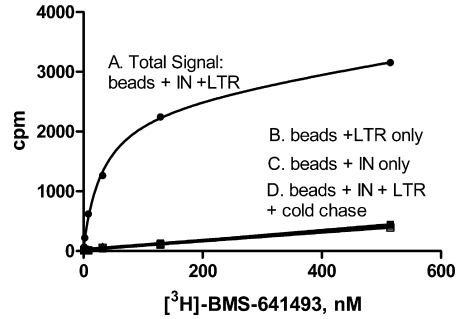

FIGURE 6: Specificity of binding of [^{3}H]-**1**. A serial dilution of [^{3}H]-1 was added to the different conditions. Assembly of integrase with all components (beads + LTR DNA + integrase) (A) produced a specific, saturable signal. Beads + LTR DNA (B), beads + integrase only (C), and beads + integrase + LTR DNA + a cold chase of 40 μM of unlabeled inhibitor **1** (D) produced identical background binding. B, C, and D data are coincident on the graph. Beads = scintillation proximity beads, as described in Experimental Procedures.

exin-1 receptor immobilized on SPA beads gave comparable rate constants to those obtained by measuring binding kinetics to the receptor on whole cells (*46*).

The results of this study assign a critical role to the terminal deoxyribose sugar in retarding the rate of inhibitor dissociation from the IN active site, as IN assembled with an LTR lacking the terminal 3′ adenosine had a greatly accelerated rate of inhibitor dissociation. In particular, the addition of a sugar phosphate was minimally required to restore the dissociation kinetics to a near-WT profile. These results argue for a close physical proximity between this terminal deoxyribose sugar and the STI in the inhibitor-bound state (Figure 2E), as has also been suggested by a recent CADD model (*42*). It is possible that the sugar retards dissociation by adopting a conformation which sterically blocks inhibitor egress or by virtue of a direct interaction of the sugar with the inhibitor in the bound state. It is also interesting that the terminal deoxyribose is minimally responsible for strand transfer activity of integrase (Table 1, last column), as has also been found for the Mu A transposase (*41*). This highlights similarities of these two DNA recombination systems.

This study also delineates a critical role of the 3′ terminal adenine base in slowing down the rate of association of the STI with its binding site. Deletion of this terminal base has a profound effect on accelerating the kinetics of binding, while base substitutions have intermediate effects. Consequently, we favor a model in which dA^1 exists in equilibrium between two binding conformations. In the preprocessed LTR the terminal dG^{-1}pdT^{-2} dinucleotide occupies the active site while dA^1 samples a conformation near K159 (*40*) and the phosphate backbone of the LTR. Immediately following 3′-processing, the active site is left open and accessible for STI binding (Figure 2B). However, after 3′-processing, the equilibrium shifts and the 3′ terminal adenine moves into the active site where it blocks access to the inhibitor binding site (Figure 2C), perhaps by acting as an internal competitive inhibitor for occupancy of that binding site or by steric interference. Such hindrance would have the effect that many of the inhibitor−enzyme complex encounters do not result in a collision required for capture (*47*). The accelerating affect produced by replacement of the adenine by cytosine or 2,6-diaminopurine indicates that these bases are less-well suited to this "blocking" function.

Prior to this study there have been no reports describing the kinetics of STI binding. In this study, we find that the kinetics of inhibitor association with IN are biexponential and best fit to a two-step binding model. It appears that the biphasic kinetics are not simply due to operating outside of pseudo-first-order conditions, as we estimate the concentration of WT binding sites to be approximately 2 nM (*16*), compared to a K_d net of 18.5 nM.

Though we cannot completely rule out heterogeneity of complexes that form under our biochemical conditions, several observations argue against this. (1) We can rule out the possibility that there are two classes of binding sites, one composed of complexes with bound LTR, one without bound LTR, as the labeled inhibitor displays no specific binding to complexes assembled in the presence of integrase but lacking any LTR DNA (Figure 6). Fully assembled complexes showed a small degree (0.15% of total cpm added) of nonspecific binding, as evidenced by a signal which was not competed off in the presence of a large molar excess of cold inhibitor. This background binding was equivalent to that observed for complexes either assembled in the absence of integrase (LTR only) or in the absence of LTR (integrase only). Thus, binding of labeled **1** to integrase in the absence of LTR DNA, though possible in principle, can be excluded under the experimental conditions employed in this study. In practice, this linear background (residual binding post cold chase dissociation) was subtracted from the kinetic data prior to analysis. (2) We observed that the kinetics of STI 1 binding were the same when assays were performed on complexes prepared over a range of integrase concentrations and with different integrase preparations. (3) The kinetic profiles of WT (and three variants) at 37 °C (Table 2) fit best to a monoexponential function derived from a one-site, one-step binding model, in contrast to the one-site, two-step fit at 20 °C. Given that both sets of data were derived from the exact same preparations of complexes, the differing kinetic profiles argue in support of an interpretation that the binding at 20 °C is truly two steps, as opposed to being an artifact of heterogeneity.

A plot of rates versus inhibitor concentration ([^{3}H]-**1**) gives a straight line fit for the faster of the two rates, and

Table 2: Rate Constants for the Binding of [H]-**1** to INs Assembled with Changes to the Terminal Adenosine at 37° C[a]

no.	LTR[b]	k_{on}, μM^{-1} s^{-1} ($\times 10^{-1}$)	k_{off}, s^{-1} ($\times 10^{-3}$)	K_d, nM[b]	k_{on} (fold over K_{on} at 20 °C)	k_{off} (fold over K_{off} at 20 °C)	K_d (fold over K_d (net) at 20 °C)
1	dC^{2}pdA^1 (WT)	0.24	0.75	31	3.0	5.0	1.7
2	dC^{2}pdC^1	2.4	0.58	2.4	5.3	4.3	0.8
3	dC^{2}pdAA^1	0.95	0.43	4.5	2.9	4.2	1.4
4	dC^{2}pdS	4.8	1.3	2.6	0.8	3.6	4.7

[a] Data is fit to a one-step binding mechanism, as described in the text. p: phosphate, d: deoxy, S: dspacer, dAA: 2,6-diaminopurine 2′-deoxyriboside. [b] $K_d = k_{off}/k_{on}$.

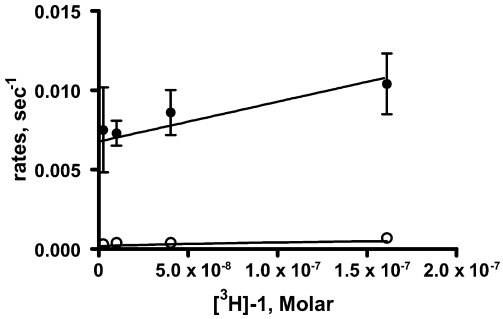

FIGURE 7: Dependence of rates on [^{3}H]-**1** binding to WT IN. Data points are from fits of binding versus time, using a biexponential equation ($N = 2$). Curves through the data points are derived from global fitting of the data following Bevilacqua et al. (*38*). Closed circles: fast component of the overall rate; open circles: slow component of the overall rate.

a hyperbolic fit for the slower rate (Figure 7). This profile is consistent with the formation of a lower affinity complex transitioning to one of higher affinity, via a slower, time-dependent step (*38*). It is revealing that removal of the 3′ terminal adenine, while leaving intact the terminal sugar phosphate, increases the overall on-rate by a factor of 78-fold, while producing only a 2.4-fold decrease in the overall rate of dissociation. The kinetics of this variant IN (dC^2 pdPS) then become consistent with a one-step binding model, implying that a step mediated by the terminal adenine, probably a conformational rearrangement delineated by some aspect of its motion (Figures 2B and 2C) relative to the inhibitor binding site, is now much faster (compare kinetic profiles, Figures 3B and 4D). Interestingly, when the kinetic data for WT IN are acquired at 37 °C (Table 2), the data best fits to a one-step binding model or possibly is composed of two steps where the second step is too rapid to be discerned with the sampling technique of this study. Therefore, conformational motions of the terminal adenosine appear to be at the borderline between relatively slow and more rapid movement over the temperature range from 20 to 37 °C.

At 37 °C, the forward and reverse rate constants for WT IN were each increased 3- and 5-fold, respectively, when compared to the composite forward (k_{on}) and reverse (k_{off}) rate constants at 20 °C (Table 2). When A^1 was substituted by 2,6-diaminopurine, cytosine, or deleted (dC^{2}pds), both the forward and reverse rate constants were increased 3−5 fold over their values at 20 °C. At 37 °C, the forward rate constants for all three LTR mutants was significantly faster than WT, with dC^{2}pds producing the largest differential (20-fold). Thus, the overall mechanistic picture at 37 °C is little changed from that at 20 °C: the terminal adenine still exerts a strong retarding effect on the kinetics of association while the terminal sugar still exerts a strong retarding effect on the kinetics of dissociation.

These findings add to our understanding of the details of the STI binding site. Our results support a model in which there is a close physical proximity of the terminal deoxyribose sugar and the inhibitor in the inhibitor-bound state. These results also demonstrate that the terminal adenine base is likely relatively close to the inhibitor binding site, as its removal greatly increases the rate of association of the inhibitor with its binding site. Finally, the relatively slow off-rates shown by this class of compounds may positively impact *in vivo* efficacy, as it suggests that the inhibitor may still be stably bound to the preintegration complex, even when the serum concentration of the drug may have fallen below that needed to inhibit virus growth. This would especially be the case for compounds that are more potent than BMS-641493, as more potent compounds with this chemotype have correspondingly slower off-rates (data not shown). The consequences of this stable binding are likely to be dead-end destruction of the preintegration complex either by cellular degradation, or the well-noted propensity of inhibited complexes to form 1 and 2-LTR circles.

ACKNOWLEDGMENT

We thank Dr. Ying-Kai Wang and Dr. Jovita Marcinkeviciene for helpful comments on the manuscript.

REFERENCES

1. LaFemina, R. L., Schneider, C. L., Robbins, H. L., Callahan, P. L., LeGrow, K., Roth, E., Schlief, W. A., and Emini, E. A. (1992) Requirement of Active Human Immunodeficiency Virus Type 1 Integrase Enzyme for Productive Infection of Human T-Lymphoi Cells. *J. Virol 66*, 7414–7419.
2. Hazuda, D. J., Felock, P., Witmer, M., Wolfe, A., Stillmock, K., Grobler, J. A., Espeseth, A., Gabryelski, L., Schleif, W., Blau, C., and Miller, M. D. (2000) Inhibitors of strand transfer that prevent integration and inhibit HIV-1 replication in cells. *Science 287*, 646–650.
3. Assante-Appiah, E., Skalka, A. M. (1999) HIV-1 integrase: structural organization, conformational changes, and catalysis, in *Advances in Virus Research*, pp 351−369, Academic Press
4. Espeseth, A. S., Felock, P., Wolfe, A., Witmer, M., Grobler, J., Anthony, N., Egbertson, M., Melamed, J. Y., Young, S., Hamill, T., Cole, J. L., and Hazuda, D. J. (2000) HIV-1 integrase inhibitors that compete with the target DNA substrate define a unique strand transfer conformation for integrase. *Proc. Natl. Acad. Sci. U.S.A. 97*, 11244–11249.
5. Pommier, Y., Johnson, A. A., and Marchand, C. (2005) Integrase inhibitors to treat HIV/Aids. *Nat. Rev. Drug Discovery 4*, 236–248.
6. Cooper, D. A., Gatell, J., Rockstroh, J., Katlama, C., Yeni, P., Lazzarin, A., Chen, J., Isaacs, R., Teppler, H., Nguyen, B.-Y., and Group, B.-S. (2007) Results of BENCHMRK-1, a Phase III study evaluating the efficacy and safey of raltegravir (MK-0518), a novel HIV-1 integrase inhibitor, in patients with triple-class resistant virus, presented at the 14th Conference on Retroviruses and Opportunistic Infections, Los Angeles, CA, p 105LB, Denver, CO, Feb 5−8, 2006.
7. Kawaguchi, I., Ishikawa, T., Ishibashi, M., Irie, S., Kakee, A. (2006) Safety and Pharmacokinetics of single oral dose of JTK-303/GS-9137, a novel HIV integrase inhibitor, in healthy volunteers, presented at the 13th Conference on Retroviruses and Opportunistic Infections (CROI), Feb 5−8, Denver, CO, Poster #580.
8. Engelman, A., Mizuuchi, K., and Craigie, R. (1991) HIV-1 DNA Integration: Mechanism of Viral DNA Cleavage and DNA Strand Transfer. *Cell 67*, 1211–1221.
9. Bushman, F. D., Fujiwara, T., and Craigie, R. (1990) Retroviral DNA Integration Directed by HIV Integration Protein in vitro. *Science 249*, 1555–1557.
10. Ellison, V., and Brown, P. O. (1994) A Stable Complex Between Integrase and Viral DNA ends Mediates Human Immunodeficiency Virus Integration in vitro. *Proc. Natl. Acad. Sci. U.S.A. 91*, 7316–7320.
11. Hazuda, D. J., Young, S. D., Guare, J. P., Anthony, N. J., Gomez, R. P., Wai, J. S., Vacca, J. P., Handt, L., Motzel, S. L., Klein, H. J., Dornadula, G., Danovich, R. M., Witmer, M. V., Wilson, K. A., Tussey, L., Schleif, W. A., Gabryelski, L. S., Jin, L., Miller, M. D., Casimiro, D. R., Emini, E. A., and Shiver, J. W. (2004) Integrase inhibitors and cellular immunity suppress retroviral replication in rhesus macaques. *Science 305*, 528–532.
12. Pais, G. C., Zhang, X., Marchand, C., Neamati, N., Cowansage, K., Svarovskaia, E. S., Pathak, V. K., Tang, Y., Nicklaus, M., Pommier, Y., and Burke, T. R., Jr. (2002) Structure Activity of

3-Aryl-1,3-diketo-Containing Compounds as HIV-1 Integrase Inhibitors(1). *J. Med. Chem. 45*, 3184–3194.
13. Marchand, C., Zhang, X., Pais, G. C., Cowansage, K., Neamati, N., Burke, T. R., Jr, and Pommier, Y. (2002) Structural Determinants for HIV-1 Integrase Inhibition by beta -Diketo Acids. *J. Biol. Chem. 277*, 12596–12603.
14. Chen, A., Weber, I. T., Harrison, R. W., and Leis, J. (2006) Identification of Amino Acids in HIV-1 and Avian Sarcoma Virus Integrase Subsites Required for Specific Recognition of the Long Terminal Repeat Ends. *J. Biol. Chem. 281*, 4173–4182.
15. Goldgur, Y., Craigie, R., Cohen, G. H., Fujiwara, T., Yoshinaga, T., Fujishita, T., Sugimoto, H., Endo, T., Murai, H., and Davies, D. R. (1999) Structure of the HIV-1 integrase catalytic domain complexed with an inhibitor: a platform for antiviral drug design. *Proc. Natl. Acad. Sci. U.S.A. 96*, 13040–13043.
16. Dicker, I. B., Samanta, H. K., Li, Z., Hong, Y., Tian, Y., Banville, J., Remillard, R. R., Walker, M. A., Langley, D. R, and Krystal, M. R. (2007) Changes To The HIV LTR And To HIV Integrase Differentially Impact HIV Integrase Assembly, Activity And The Binding Of Strand Transfer Inhibitors. *J. Biol. Chem. 282* (43), 31186–31196.
17. De Luca, L., Pedretti, A., Vistoli, G., Letizia Barreca, M., Villa, L., Monforte, P., and Chimirri, A. (2003) Analysis of the full-length integrase-DNA complex by a modified approach for DNA docking. *Biochem. Biophys. Res. Commun. 310*, 1083–1088.
18. Wang, L. D., Liu, C. L., Chen, W. Z., and Wang, C. X. (2005) Constructing HIV-1 integrase tetramer and exploring influences of metal ions on forming integrase-DNA complex. *Biochem. Biophys. Res. Commun. 337*, 313–319.
19. Karki, R. G., Tang, Y., Burke, T. R., Jr., and Nicklaus, M. C. (2004) Model of full-length HIV-1 integrase complexed with viral DNA as template for anti-HIV drug design. *J. Comput.-Aided Mol. Des. 18*, 739–760.
20. Wielens, J., Crosby, I. T., and Chalmers, D. K. (2005) A three-dimensional model of the human immunodeficiency virus type 1 integration complex. *J. Comput.-Aided Mol. Des. 19*, 301–317.
21. Gao, K., Butler, S. L., and Bushman, F. (2001) Human immunodeficiency virus type 1 integrase: arrangement of protein domains in active cDNA complexes. *EMBO J. 20*, 3565–3576.
22. Bourke, D. G., Chalmers, D. K., Jones, R. D., Crosby, I. T., and Wielens, J. (2001) Molecular modeling of inhibitors in the active site of HIV-1 integrase, presented at the 14th International Conference on Antivirus Research, Seattle, WA, April, 2001.
23. Grobler, J. A., Stillmock, K., Hu, B., Witmer, M., Felock, P., Espeseth, A. S., Wolfe, A., Egbertson, M., Bourgeois, M., Melamed, J., Wai, J. S., Young, S., Vacca, J., and Hazuda, D. J. (2002) Diketo acid inhibitor mechanism and HIV-1 integrase: Implications for metal binding in the active site of phosphotransferase enzymes. *Proc. Natl. Acad. Sci. U.S.A. 99*, 6661–6666.
24. Marchand, C., Johnson, A. A., Karki, R. G., Pais, G. C., Zhang, X., Cowansage, K., Patel, T. A., Nicklaus, M. C, Burke, T. R, Jr., and Pommier, Y. (2003) Metal-dependent inhibition of HIV-1 integrase by beta-diketo acids and resistance of the soluble double-mutant (F185K/C280S). *Mol. Pharmacol. 64*, 600–609.
25. Maurin, C., Bailly, F., Buisine, E., Vezin, H., Mbemba, G., Mouscadet, J. F., and Cotelle, P. (2004) Spectroscopic Studies of Diketoacids−Metal Interactions. A Probing Tool for the Pharmacophoric Intermetallic Distance in the HIV-1 Integrase Active Site. *J. Med. Chem. 47*, 5583–5586.
26. Sotriffer, C. A., Ni, H., and McCammon, J. A. (2000) Active site binding modes of HIV-1 integrase inhibitors. *J. Med. Chem. 43*, 4109–4117.
27. Carlson, H. A., Masukawa, K. M., Rubins, K., Bushman, F. D., Jorgensen, W. L., Lins, R. D., Briggs, J. M., and McCammon, J. A. (2000) Developing a dynamic pharmacophore model for HIV-1 integrase. *J. Med. Chem. 43*, 2100–2114.
28. Barreca, M. L., DeLuca, L., Iraci, N., and Chimirri, A. (2006) Binding Mode Prediction of Strand Transfer HIV-1 Integrase Inhibitors Using Tn5 Transposase as a Plausible Surrogate Model for HIV-1 Integrase. *J. Med. Chem. 49* (13), 3994–3997.
29. Cox, A. G., and Nair, V. (2006) Novel HIV integrase inhibitors with anti-HIV activity: insights into integrase inhibition from docking studies. *Antiviral Chem. Chemother. 17*, 343–353.
30. Fikkert, V., Van Maele, B., Vercammen, J., Hantson, A., Van Remoortel, B., Michiels, M., Gurnari, C., Pannecouque, C., De Maeyer, M., Engelborghs, Y., De Clercq, E., Debyser, Z., and Witvrouw, M. (2003) Development of Resistance against Diketo Derivatives of Human Immunodeficiency Virus Type 1 by Progressive Accumulation of Integrase Mutations. *J. Virol. 77*, 11459–11470.
31. King, P. J., Lee, D. J., Reinke, R. A., Victoria, J. G., Beale, K., and Robinson, W. E. (2003) Human immunodeficiency virus type-1 integrase containing a glycine to serine mutation at position 140 is attenuated for catalysis and resistant to integrase inhibitors. *Virology 306*, 147–161.
32. Fikkert, V., Hombrouck, A., Van Remoortel, B., De Maeyer, M., Pannecouque, C., De Clercq, E., Debyser, Z., and Witvrouw, M. (2004) Multiple mutations in human immunodeficiency virus-1 integrase confer resistance to the clinical trial drug S-1360. *AIDS 18*, 2019–2020.
33. Hazuda, D. J., Anthony, N. J., Gomez, R. P., Jolly, S. M., Wai, J. S., Zhuang, L., Fisher, T. E., Embrey, M., Guare, J. P, Jr., Egbertson, M. S., Vacca, J. P., Huff, J. R., Felock, P. J., Witmer, M. V., Stillmock, K. A., Danovich, R., Grobler, J., Miller, M. D., Espeseth, A. S., Jin, L., Chen, I. W., Lin, J. H., Kassahun, K., Ellis, J. D., Wong, B. K., Xu, W., Pearson, P. G., Schleif, W. A., Cortese, R., Emini, E., Summa, V., Holloway, M. K., and Young, S. D. (2004) A naphthyridine carboxamide provides evidence for discordant resistance between mechanistically identical inhibitors of HIV-1 integrase. *Proc. Natl. Acad. Sci. U.S.A. 101*, 11233–11238.
34. Herring, B. L., Cunningham, A. L., and Dwyer, D. E. (2004) Potential Drug Resistance Polymorphisms in the Integrase Gene of HIV Type 1 Subtype A. *AIDS Res. Hum. Retroviruses 20*, 1010–1014.
35. Lee, D. J., and Robinson, W. E., Jr. (2004) Human Immunodeficiency Virus Type 1 (HIV-1) Integrase: Resistance to Diketo Acid Integrase Inhibitors Impairs HIV-1 Replication and Integration and Confers Cross-Resistance to L-Chicoric Acid. *J. Virol. 78*, 5835–5847.
36. Kehlenbeck, S., Betz, U., Birkmann, A., Fast, B., Goller, A. H., Henninger, K., Lowinger, T., Marrero, D., Paessens, A., Paulsen, D., Pevzner, V., Schohe-Loop, R., Tsujishita, H., Welker, R., Kreuter, J., Rubsamen-Waigmann, H., and Dittmer, F. (2006) Dihydroxythiophenes are novel potent inhibitors of human immunodeficiency virus integrase with a diketo acid-like pharmacophore. *J. Virol. 80*, 6883–6894.
37. Lee, D. J., and Robinson, W. E., Jr. (2006) Preliminary mapping of a putative inhibitor-binding pocket for human immunodeficiency virus type 1 integrase inhibitors. *Antimicrob. Agents Chemother. 50*, 134–142.
38. Bevilacqua, P., Kierzek, R., Johnson, K. A., and Turner, D. H. (1992) Dynamics of Ribozyme Binding of Substrate Revealed by Fluorescence-Directed Stopped-Flow Methods. *Science 258*, 1355–1358.
39. Pandey, K., Bera, S., Zahm, J., Vora, A., Stillmock, K., Hazuda, D., and Grandgenett, D. (2007) Inhibition of human immunodeficiency virus type 1 concerted integration by strand transfer inhibitors which recognize a transient structural intermediate. *J. Virol. 81*, 12189–12199.
40. Jenkins, T. M., Esposito, D., Engelman, A., and Craigie, R. (1997) Critical contacts between HIV-1 integrase and viral DNA identified by structure-based analysis and photo-crosslinking. *EMBO J. 16*, 6849–6859.
41. Goldhaber-Gordon, I., Early, M. H., and Baker, T. A. (2003) The terminal nucleotide of the Mu genome controls catalysis of DNA strand transfer. *Proc. Natl. Acad. Sci. U.S.A. 100*, 7509–7514.
42. Chen, X., Tsiang, M., Yu, F., Hung, M., Jones, G. S., Zeynalzadegan, A., Qi, X, Jin, H., Kim, C. U., Swaminathan, S., and Chen, J. M. (2008) Modeling, Analysis, and Validation of a Novel HIV Integrase Structure Provide Insights into the Binding Modes of Potent Integrase Inhibitors. *J. Mol. Biol. 380*, 504–519.
43. Alderton, W. K., Boyhan, A., and Lowe, P. N. (1998) Nitroarginine and tetrahydrobiopterin binding to the haem domain of neuronal nitric oxide synthase using a scintillation proximity assay. *Biochem. J. 332*, 195–201.
44. Furfine, E. S., Harmon, M. F., and Paith, J. E. (1993) Selective inhibition of constitutive nitric oxide synthase by L-NG-nitroarginine. *Biochemistry 32*, 8512–8517.
45. Gorren, A. C. F., Schrammel, A., Schmidt, K., and Mayer, B. 1998Effects of pH on the structure and function of neuronal nitric oxide synthase*Biochem. J. 331*, 801–807.
46. Langmead, C. J., Jerman, J. C., Brough, S. J., Scott, C., Porter, R. A., and Herdon, H. J. (2004) Characterisation of the binding of [3H]-SB-674042, a novel nonpeptide antagonist, to the human orexin-1 receptor. *Br. J. Pharmacol. 141*, 340–346.
47. North, A. M. (1964)*The Collision Theory of Chemical Reactions in Liquids*, pp 258−259, Methuen, London.

BI801372D